

# Anomalous Early Triassic sediment fluxes due to elevated weathering rates and their biological consequences

Thomas J. Algeo<sup>1\*</sup> and Richard J. Twitchett<sup>2</sup>

<sup>1</sup>Department of Geology, University of Cincinnati, Cincinnati, Ohio 45221, USA

<sup>2</sup>School of Geography, Earth & Environmental Sciences, University of Plymouth, Plymouth PL4 8AA, UK

## ABSTRACT

Analysis of 16 marine Permian-Triassic boundary sections with a near-global distribution demonstrates systematic changes in sediment fluxes and lithologies in the aftermath of the end-Permian crisis. Sections from continent-margin and platform settings exhibit higher bulk accumulation rates (BARs) and more clay-rich compositions in the Griesbachian (earliest Triassic) relative to the Changhsingian (latest Permian). These patterns, which largely transcend regional variations in tectonic setting, sequence stratigraphic factors, and facies, are hypothesized to have resulted from a substantial (average  $\sim 7\times$ ) increase in the flux of eroded material from adjacent land areas owing to accelerated rates of chemical and physical weathering as a function of higher surface temperatures, increased acidity of precipitation, and changes in landscape stability tied to destruction of terrestrial ecosystems. This sediment surge may have been a contributory factor to the latest Permian marine biotic crisis as well as to the delayed recovery of Early Triassic marine ecosystems owing to the harmful effects of siltation and eutrophication. Contemporaneous deep-sea sections show no increases in sediment flux across the Permian-Triassic boundary owing to their remoteness from continental siliciclastic sources and location below the paleo-carbonate compensation depth.

## INTRODUCTION

The  $\sim 252$ -m.y.-old latest Permian mass extinction event represents the largest biotic crisis in the Phanerozoic record, during which  $\sim 90\%$  of marine invertebrate species died out (Erwin et al., 2002). Terrestrial ecosystems were also devastated, resulting in major extinctions among tetrapods (Retallack, 1995) and a shift from gymnosperm-dominated floras to rapidly growing, early successional communities dominated by lycopsids and ferns (Looy et al., 2001). Widespread loss of vegetative cover is thought to have led to massive soil erosion, as shown by a shift from fine-grained meandering to conglomeratic braided fluvial facies (Newell et al., 1999; Ward et al., 2000), by redeposition of soil clasts (Retallack, 2005), and by increased sedimentation rates in terrestrial successions (Retallack, 1999). Although the signature of this erosional event has been recognized in marine successions in the form of soil-derived biomarkers (Sephton et al., 2005; Xie et al., 2007), the scale and consequences of a massive transfer of mineral and organic matter from the terrestrial to the marine realm have not been fully recognized or explored to date. For example, average linear sedimentation rates (LSRs) at Meishan in eastern China increased from 10–18 m m.y.<sup>-1</sup> in the Lopingian (Upper Permian) to 105–488 m m.y.<sup>-1</sup> in the Induan-Olenekian (Lower Triassic; Fig. 1). LSRs increased by a smaller, yet still substantial amount (from 6–11 m m.y.<sup>-1</sup> to 31–89 m m.y.<sup>-1</sup>) at Chaohu,  $\sim 180$  km downramp from Meishan (Fig. 1), showing that sediment delivery was focused on shallow-marine shelves adjacent to landmasses, consistent with derivation through subaerial weathering. Such large increases in sediment flux must have profoundly affected marine ecosystems through higher nutrient availability, increased turbidity, and smothering of benthic organisms. In this contribution, we examine evidence for a surge in sediment delivery to Early Triassic

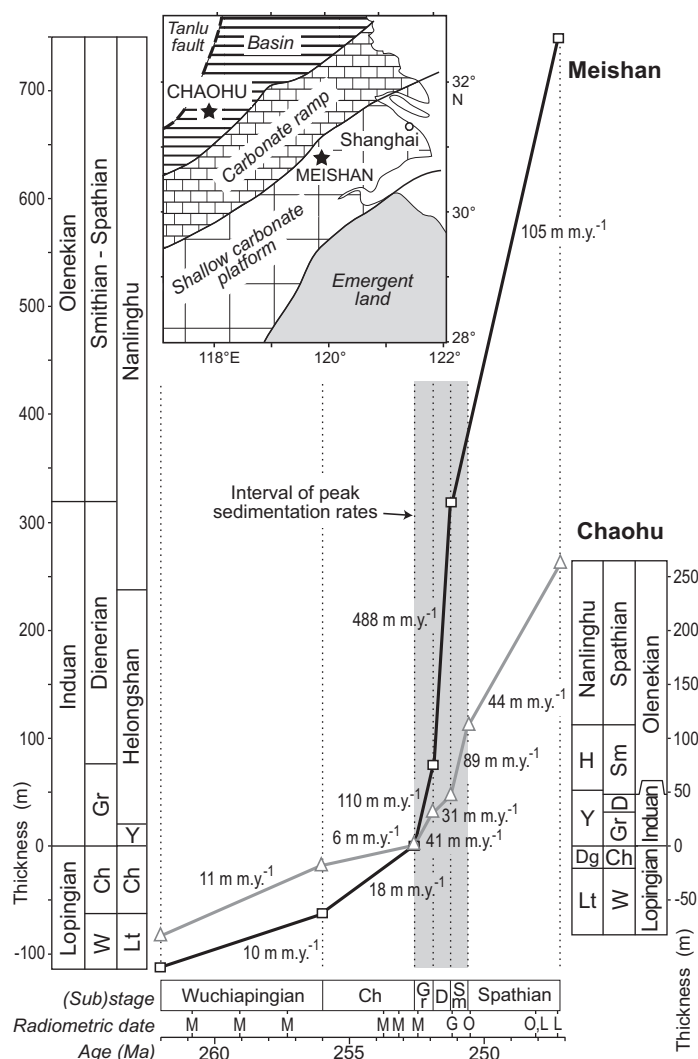


**Figure 1.** Late Permian–Early Triassic sedimentation rates and (inset) paleogeography for Meishan and Chaohu, eastern China. Note sedimentation rate peak during Griesbachian to Smithian sub-stages. Abbreviations: M—Mundil et al. (2004); G—Galfetti et al. (2007); O—Ovtcharova et al. (2006); L—Lehrmann et al. (2006); Ch—Changhsingian, D—Dienerian, Gr—Griesbachian, Sm—Smithian, W—Wuchiapingian, Dg—Dalong Formation, H—Helonghsan Formation, Lt—Longtan Formation, Y—Yinkeng Formation.

marine depositional systems and its possible effects on contemporaneous marine biotas.

## METHODS

This study focuses on changes in LSRs from the Changhsingian (latest Permian) to the Griesbachian (earliest Triassic, but including post-crisis strata of latest Changhsingian age). LSRs (units of m m.y.<sup>-1</sup>) were calculated for each study section as the full thickness of a given

\*E-mail: Thomas.Algeo@uc.edu.

time-stratigraphic unit divided by the duration of that unit (Table DR1 in the GSA Data Repository<sup>1</sup>). Bulk accumulation rates (BARs) were calculated as LSR multiplied by bulk sediment density, and fluxes of sediment components (i.e.,  $\text{CaCO}_3$ , quartz, and clays) were calculated as BAR multiplied by percent abundance of each sediment fraction (units of  $\text{g cm}^{-3}$ ; Table DR2). The lithologic composition of each study section was calculated from elemental data (Table DR3; see the Methods section of the Data Repository for details). Age constraints for rate calculations were provided by recent chemical abrasion–thermal ionization mass spectrometry (CA-TIMS) studies of U–Pb in zircons (Mundil et al., 2004; Ovtcharova et al., 2006; Galfetti et al., 2007; Lehrmann et al., 2006), from which the ages of the Wuchiapingian–Changhsingian, Changhsingian–Induan (or Permian–Triassic), and Induan–Olenekian stage boundaries were estimated at  $256.0 \pm 1.0$  Ma,  $252.6 \pm 0.2$  Ma, and  $251.3 \pm 0.2$  Ma, respectively. These dates yield durations for the Changhsingian and Induan stages of  $3.4 \pm 1.2$  m.y. and  $1.3 \pm 0.4$  m.y., respectively, with the duration of the Griesbachian substage of the Induan stage estimated at  $0.7 \pm 0.4$  m.y. (See the Methods section of the Data Repository for additional information.)

## RESULTS

The 16 study sections allow assessment of global patterns of sedimentation across the Permian–Triassic boundary owing to their wide geographic distribution: 1–7 from the Neotethys, 8–9 from the Paleotethys, 10–14 from the northern and western margins of Pangea, and 15–16 from Panthalassa (see Tables DR1–DR3 for section identification). BARs increase sharply from the Changhsingian (mostly  $<100 \text{ g m}^{-2} \text{ yr}^{-1}$ ) to the Griesbachian (mostly  $200\text{--}600 \text{ g m}^{-2} \text{ yr}^{-1}$ ), with a mean global increase of  $\sim 7\times$  or  $700\%$  (Fig. 2; Table DR2). Early Triassic BARs are high for both carbonate-dominated Neotethyan and siliciclastic-dominated northern and western Pangean sections, but values are lower for Paleotethyan and Panthalassic sections. All sections but one (8) show a shift toward a more clay-rich composition in the Griesbachian, with increases of  $+5\%$ – $10\%$  in carbonate-dominated sections and increases of  $+10\%$ – $35\%$  in mixed and siliciclastic-dominated sections (Fig. 3; Table DR3).

## DISCUSSION

### Dating Uncertainties

Uncertainties in the estimated durations of the Changhsingian ( $3.4 \pm 1.2$  m.y.) and Griesbachian ( $0.7 \pm 0.4$  m.y.) can account at most for only a fraction of the anomalous increases in sedimentation rates across the Permian–Triassic boundary. Adopting a minimum duration of 2.2 m.y. for the Changhsingian and a maximum duration of 1.1 m.y. for the Griesbachian, rate differences are reduced by a factor of only  $2.5\times$  [i.e.,  $(3.4/0.7)/(2.2/1.1)$ ], which still yields rates that are at least  $\sim 3\times$  higher (i.e.,  $7\times/2.5\times$ ) on average for the Griesbachian relative to the Changhsingian. Further, a 1.1 m.y. duration for the Griesbachian appears unlikely in view of Mundil et al.'s (2010) estimate of 1.0 m.y. for the entire Induan Stage. Thus, unless there are major, unrecognized errors associated with recent radiometric dating studies of the Permian–Triassic, sedimentary fluxes were much higher in the Griesbachian than in the Changhsingian.

### Sequence Stratigraphic and Tectonic Controls on Sedimentation

Eustatic elevations rose during the earliest Triassic in response to climatic warming (Hallam and Wignall, 1999), although the magnitude of

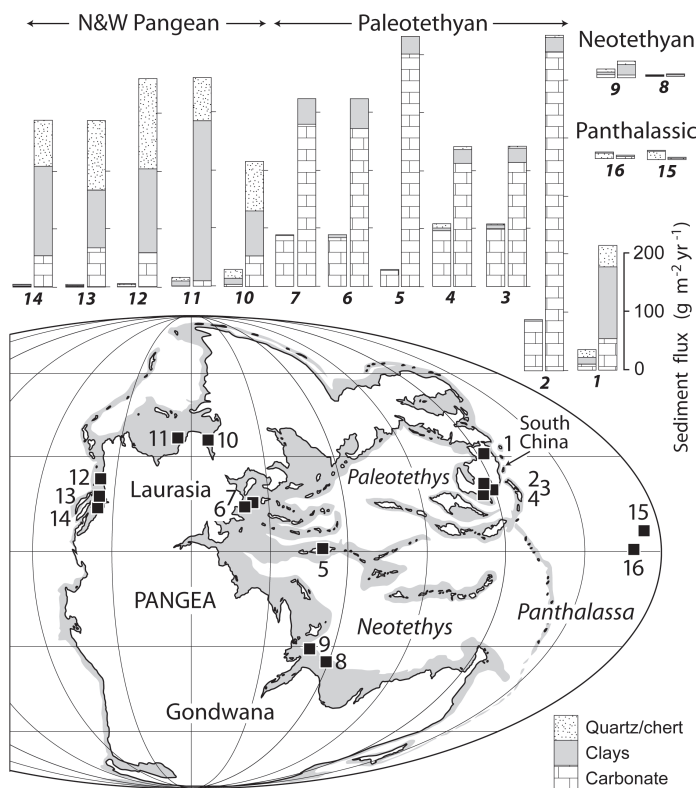


**Figure 2.** Change in sediment fluxes across Permian–Triassic boundary (PTB); for each study section, left and right columns represent Changhsingian and Griesbachian, respectively (Table DR2 [see footnote 1]). Note vertical scale at right in units of  $\text{g m}^{-2} \text{ yr}^{-1}$  and lithologic key in lower right. Base map is from Ron Blakey (<http://jan.ucc.nau.edu/~rcb7/>).

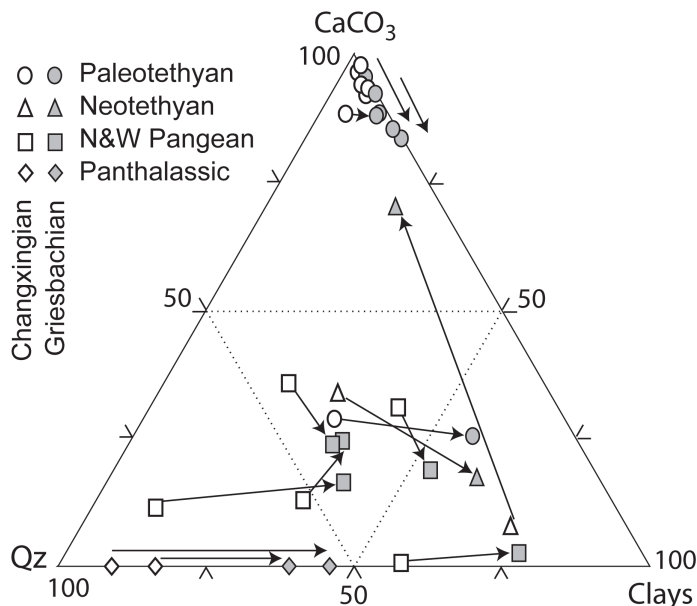


**Figure 3.** Change in mineralogic composition across Permian–Triassic boundary (PTB); for each study section, Changhsingian and Griesbachian units are shown as open and solid symbols, respectively, and are connected by an arrow (Table DR3 [see footnote 1]). Quartz (Qz) apex includes both detrital and biogenic silica.

<sup>1</sup>GSA Data Repository item 2010283, methods, Figure DR1 (Late Permian–Early Triassic time scale), Table DR1 (linear sedimentation rates for study sections), Table DR2 (sediment fluxes for study sections), Table DR3 (lithologic compositions of study sections), and Table DR4 (biological effects of sedimentation), is available online at [www.geosociety.org/pubs/ft2010.htm](http://www.geosociety.org/pubs/ft2010.htm), or on request from [editing@geosociety.org](mailto:editing@geosociety.org) or Documents Secretary, GSA, P.O. Box 9140, Boulder, CO 80301, USA.

this rise was probably small ( $\leq 20$  m) owing to the limited mass of continental ice at that time. A eustatic rise would have created accommodation space and might account for a general shift toward higher clay concentrations (Fig. 3) if (1) coarser siliciclastics were trapped in receding paralic facies, and (2) drowning reduced rates of shallow-marine carbonate production. However, both of these effects should have been accompanied by a reduction in BARs, rather than an increase, as actually observed (Fig. 2). The observation that BARs increased in conjunction with a shift toward more clay-rich compositions in both siliciclastic and carbonate facies during the Early Triassic indicates that a eustatic rise alone is insufficient to account for changes in sedimentary rates and patterns across the Permian-Triassic boundary.

Assuming only a modest eustatic rise during the Early Triassic, sedimentation rates of  $>100$  m  $\text{m.y.}^{-1}$  (Fig. 1) would appear to create an accommodation space problem. However, isostatic crustal adjustments in response to (un)loading associated with continental glaciation (Peltier, 1987) and erosion (Opdyke et al., 1984) are rapid ( $10^3$ – $10^5$  yr) relative to the duration of the study interval ( $>10^6$  yr). Further, cratonic uplift and subsidence are generally balanced around a fulcrum (or “tectonic hinge”) that is commonly stable at time scales of a few million years (Allen and Allen, 2005), so enhanced rates of sediment erosion and transport during the Early Triassic would have simply accelerated motion around such fulcrum. Tectonic factors had a local influence on study-section BARs and lithologies. Rifting along the northern Gondwanan margin produced isolated crustal blocks in the Paleotethys during the Permian-Triassic, limiting detrital influx to sections 8 and 9 (see references in Algeo et al., 2007), and Panthalassic deep-sea sections (15–16) show lower BARs during the Early Triassic owing to a reduction in biogenic silica flux without an increase in detrital flux because of their distance from continental siliciclastic sources (Algeo et al., 2010).

Increased sediment fluxes during the Early Triassic cannot have been due solely to soil erosion. Stripping of a 1-m-thick soil layer from continents (modern area =  $148.6 \times 10^6$  km<sup>2</sup>) yields an average thickness of only 5.5 m of sediment on continental shelves ( $26.8 \times 10^6$  km<sup>2</sup>). Because the Lower Triassic is several hundred meters thick in most areas, soil erosion can account for only a fraction of this material (probably the few meters around the Permian-Triassic boundary containing soil biomarkers; e.g., Sephton et al., 2005), and the remainder must represent increased rates of bedrock weathering. The shift toward more clay-rich compositions in most regions (Fig. 3) suggests a relative increase in chemical over physical weathering rates (cf. Sheldon, 2006). Such a pattern could reflect intensified weathering due to (1) higher temperatures (Retallack, 1999), accelerating reaction rates, (2) higher levels of atmospheric CO<sub>2</sub> and SO<sub>2</sub> (Wignall, 2007), increasing the acidity of precipitation, and (3) increased exposure of fresh bedrock following terrestrial ecosystem destruction and soil erosion. Sedimentation rate changes were closely linked to changes in terrestrial ecosystems, with accelerated erosion following decimation of forests in the latest Permian (Looy et al., 2001) and reduced erosion coinciding with regrowth of forests in the late Olenekian (Looy et al., 1999).

### Biotic Consequences of Enhanced Sediment Fluxes

An influx of detrital sediment to Early Triassic freshwater and marine ecosystems would have had profound biological consequences (Fig. 4). At the organismal level, elevated turbidity causes a reduction in feeding activity, osmoregulation, growth rate, body size, larval recruitment, development, and survival (Table DR4). Suspension feeders suffer because of reduced seston quality and the elevated energy costs involved in the removal of inorganic particles. Grazers suffer if sediment influx is great enough to bury and kill off their food source. Most plants are adversely affected by reduced light levels, although some fast-growing organisms (e.g., turf algae) achieve a competitive advantage under such conditions. Even predatory organisms such as fish can be affected through physical

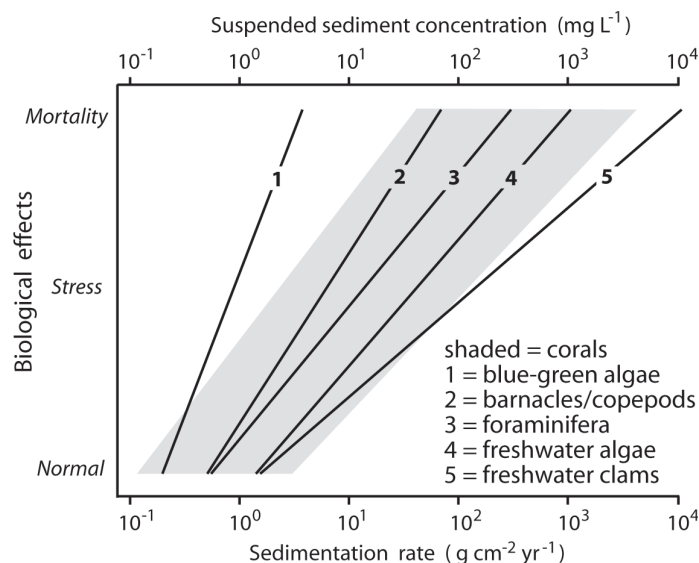


**Figure 4. Biological effects of increased suspended sediment concentrations (upper scale) or sedimentation rates (lower scale). General clade-related patterns: greater vulnerability of marine organisms relative to freshwater species, autotrophs relative to heterotrophs, and sessile taxa relative to mobile ones. Relationships are approximate; data and sources given in Table DR4 (see footnote 1).**

damage to gills, increased susceptibility to disease, and altered feeding behavior. Patterns of differential survival in the Early Triassic may reflect varying vulnerability to sediment fluxes as a function of trophic mode, e.g., lower extinction rates among deposit-feeding holothurians relative to suspension-feeding crinoids (Twitchett and Oji, 2005). Although the resilience of aquatic organisms to sediment influx is clade- and taxon-specific, experimental and observational studies have shown that flux increases of 5–20 $\times$  induce biotic stress and increases of 20–100 $\times$  generally result in mortality (Fig. 4).

Enhanced chemical weathering during the Early Triassic may have led to other harmful effects related to high inorganic nutrient (N and P) concentrations, e.g., lower rates of skeletal calcification, lower rates of fertilization and larval survival, and decreased resistance to borers and disease among corals (Table DR4). Elevated nutrient levels can also promote polymer production by particle-attached microorganisms in the water column, leading to flocculation and rapid particle settling (“marine snow”), a process that smothers benthic organisms (Fabricius and Wolanski, 2000). Consequent changes in substrate consistency may have favored organisms adapted to soft, unstable substrates (e.g., “paper pectens” such as *Claraia*) and reduced ecological tiering in Early Triassic marine ecosystems (Fraiser and Bottjer, 2005).

At the ecosystem level, increased sediment fluxes commonly result in biodiversity losses and reduced ecosystem resilience (Table DR4; Fabricius, 2005, and references therein). Modern marine ecosystems subject to sediment stress develop an unusual community structure characterized by high abundance, low diversity, very small body sizes, and dominance of small, infaunal deposit-feeding polychaetes (Smith and Kukert, 1996). Most Early Triassic marine ecosystems had a similar community structure and an ichnofauna that was dominated by *Planolites*, a probable trace of deposit-feeding polychaetes (Twitchett, 1999, 2007). Resilience to high sediment fluxes depends in part on the duration of exposure, since biotic stress correlates positively with time-integrated exposure (i.e., duration times flux) in experimental studies (Philipp and Fabricius, 2003). The harmful effects of detrital sedimentation on Early Triassic marine



ecosystems may have been particularly severe given that sedimentation rates were elevated during much of the >1-m.y.-long Induan Stage and coincided with other debilitating factors such as elevated temperatures, benthic anoxia, and hypercapnia (Knoll et al., 2007).

## CONCLUSIONS

From the Changhsingian (latest Permian) to the Griesbachian (earliest Triassic), sediment fluxes to marine depositional systems increased by an average of ~700% and became more clay-rich globally. These changes reflect elevated rates of continental erosion and a relative increase in chemical over physical weathering as a consequence of higher temperatures, increased acidity of precipitation, and changes in landscape stability following the end-Permian devastation of terrestrial ecosystems. High sediment fluxes were sustained during most of the Early Triassic and may have been an important factor in the delayed recovery of marine ecosystems at that time.

## ACKNOWLEDGMENTS

This project was supported by grants to Algeo from the National Science Foundation (grants EAR-0618003 and EAR-0745574). This paper is a contribution to International Geoscience Programme Project 572.

## REFERENCES CITED

Algeo, T.J., Hannigan, R., Rowe, H., Brookfield, M., Baud, A., Krystyn, L., and Ellwood, B.B., 2007, Sequencing events across the Permian-Triassic boundary, Guryul Ravine (Kashmir, India): Palaeogeography, Palaeoclimatology, Palaeoecology, v. 252, p. 328–346, doi: 10.1016/j.palaeo.2006.11.050.

Algeo, T.J., Hinnov, L., Moser, J., Maynard, J.B., Elswick, E., Kuwahara, K., and Sano, H., 2010, Changes in productivity and redox conditions in the Panthalassic Ocean during the latest Permian: *Geology*, v. 38, p. 187–190, doi: 10.1130/G30483.1.

Allen, P.A., and Allen, J.R., 2005, *Basin Analysis: Principles and Applications* (2nd ed.): Oxford, Blackwell, 560 p.

Erwin, D.H., Bowring, S.A., and Jin, Y.-G., 2002, End-Permian mass-extinctions: A review, in Koeberl, C., and MacLeod, K.G., eds., *Catastrophic Events and Mass Extinctions: Impacts and Beyond*: Geological Society of America Special Paper 356, p. 353–383.

Fabricius, K.E., 2005, Effects of terrestrial runoff on the ecology of corals and coral reefs: Review and synthesis: *Marine Pollution Bulletin*, v. 50, p. 125–146, doi: 10.1016/j.marpolbul.2004.11.028.

Fabricius, K.E., and Wolanski, E., 2000, Rapid smothering of coral reef organisms by muddy marine snow: *Estuarine, Coastal and Shelf Science*, v. 50, p. 115–120, doi: 10.1006/ecss.1999.0538.

Fraiser, M.L., and Bottjer, D.J., 2005, Restructuring in benthic level–bottom shallow marine communities due to prolonged environmental stress following the end-Permian mass extinction: *Comptes Rendus, Palévol*, v. 4, p. 515–523.

Galfetti, T., Bucher, H., Ovtcharova, M., Schaltegger, U., Brayard, A., Brühwiler, T., Goudemand, N., Weissert, H., Hochuli, P.A., Cordey, F., and Guodun, K., 2007, Timing of the Early Triassic carbon cycle perturbations inferred from new U-Pb ages and ammonoid biochronozones: *Earth and Planetary Science Letters*, v. 258, p. 593–604, doi: 10.1016/j.epsl.2007.04.023.

Hallam, A., and Wignall, P.B., 1999, Mass extinctions and sea-level changes: *Earth-Science Reviews*, v. 48, p. 217–250, doi: 10.1016/S0012-8252(99)00055-0.

Knoll, A.H., Bambach, R.K., Payne, J.L., Pruss, S., and Fischer, W.W., 2007, Paleophysiology and end-Permian mass extinction: *Earth and Planetary Science Letters*, v. 256, p. 295–313, doi: 10.1016/j.epsl.2007.02.018.

Lehrmann, D.J., Ramezani, J., Bowring, S.A., Martin, M.W., Montgomery, P., Enos, P., Payne, J.L., Orchard, M.J., Wang, H., and Wei, J., 2006, Timing of recovery from the end-Permian extinction: Geochronologic and biostratigraphic constraints from south China: *Geology*, v. 34, p. 1053–1056, doi: 10.1130/G22827A.1.

Looy, C.V., Brugman, W.A., Dilcher, D.L., and Visscher, H., 1999, The delayed resurgence of equatorial forests after the Permian-Triassic ecological crisis: *Proceedings of the National Academy of Sciences of the United States of America*, v. 96, p. 13,857–13,862, doi: 10.1073/pnas.96.24.13857.

Looy, C.V., Twitchett, R.J., Dilcher, D.L., van Konijnenburg-van Cittert, J.H.A., and Visscher, H., 2001, Life in the end-Permian dead zone: *Proceedings of*

the National Academy of Sciences of the United States of America, v. 98, p. 7879–7883, doi: 10.1073/pnas.131218098.

Mundil, R., Ludwig, K.R., Metcalfe, I., and Renne, P.R., 2004, Age and timing of the Permian mass extinctions: U/Pb dating of closed-system zircons: *Science*, v. 305, p. 1760–1763, doi: 10.1126/science.1101012.

Mundil, R., Pálffy, J., Renne, P.R., and Brack, P., 2010, The Triassic time scale: New constraints and a review of geochronological data, in Lucas, S.G., ed., *The Triassic Timescale*: Geological Society of London Special Publication 334, p. 41–60.

Newell, A.J., Tverdokhlebov, V.P., and Benton, M.J., 1999, Interplay of tectonics and climate on a transverse fluvial system, Upper Permian, southern Uralian foreland basin, Russia: *Sedimentary Geology*, v. 127, p. 11–29, doi: 10.1016/S0037-0738(99)00009-3.

Opdyke, N., Spangler, D., Smith, D., Jones, R., and Lindquist, R., 1984, Origin of the epeirogenic uplift of Pliocene-Pleistocene beach ridges in Florida and development of the Florida karst: *Geology*, v. 12, p. 226–228.

Ovtcharova, M., Bucher, H., Schaltegger, U., Galfetti, T., Brayard, A., and Guex, J., 2006, New Early to Middle Triassic U-Pb ages from South China: Calibration with ammonoid biochronozones and implications for the timing of the Triassic biotic recovery: *Earth and Planetary Science Letters*, v. 243, p. 463–475, doi: 10.1016/j.epsl.2006.01.042.

Peltier, W.R., 1987, Glacial isostasy, mantle viscosity, and Pleistocene climatic change, in Ruddiman, W.F., and Wright, H.E., eds., *North America and Adjacent Oceans*: Boulder, Colorado, Geological Society of America, *The Geology of North America*, vol. K-3, p. 155–181.

Philipp, E., and Fabricius, K., 2003, Photophysiological stress in scleractinian corals in response to short-term sedimentation: *Journal of Experimental Marine Biology and Ecology*, v. 287, p. 57–78, doi: 10.1016/S0022-0981(02)00495-1.

Retallack, G.J., 1995, Permian-Triassic extinction on land: *Science*, v. 267, p. 77–80, doi: 10.1126/science.267.5194.77.

Retallack, G.J., 1999, Postapocalyptic greenhouse paleoclimate revealed by earliest Triassic paleosols in the Sydney Basin, Australia: *Geological Society of America Bulletin*, v. 111, p. 52–70, doi: 10.1130/0016-7606(1999)111<0052:PGPRBE>2.3.CO;2.

Retallack, G.J., 2005, Earliest Triassic claystone breccias and soil-erosion crisis: *Journal of Sedimentary Research*, v. 75, p. 679–695, doi: 10.2110/jsr.2005.055.

Sephton, M.A., Looy, C.V., Brinkhuis, H., Wignall, P.B., de Leeuw, J.W., and Visscher, H., 2005, Catastrophic soil erosion during the end-Permian biotic crisis: *Geology*, v. 33, p. 941–944, doi: 10.1130/G21784.1.

Sheldon, N.D., 2006, Abrupt chemical weathering increase across the Permian-Triassic boundary: *Palaeogeography, Palaeoclimatology, Palaeoecology*, v. 231, p. 315–321.

Smith, C.R., and Kukert, H., 1996, Macrobenthic community structure, secondary production, and rates of bioturbation and sedimentation at the Kaneohe Bay lagoon floor: *Pacific Science*, v. 50, p. 211–229.

Twitchett, R.J., 1999, Palaeoenvironments and faunal recovery after the end-Permian mass extinction: *Palaeogeography, Palaeoclimatology, Palaeoecology*, v. 154, p. 27–37, doi: 10.1016/S0031-0182(99)00085-1.

Twitchett, R.J., 2007, The Lilliput effect in the aftermath of the end-Permian extinction event: *Palaeogeography, Palaeoclimatology, Palaeoecology*, v. 252, p. 132–144, doi: 10.1016/j.palaeo.2006.11.038.

Twitchett, R.J., and Oji, T., 2005, Early Triassic recovery of echinoderms: *Comptes Rendus, Palévol*, v. 4, p. 531–542, doi: 10.1016/j.crpv.2005.02.006.

Ward, P.D., Montgomery, D.R., and Smith, R., 2000, Altered river morphology in South Africa related to the Permian-Triassic extinction: *Science*, v. 289, p. 1740–1743, doi: 10.1126/science.289.5485.1740.

Wignall, P.B., 2007, The end-Permian mass extinction—How bad did it get?: *Geobiology*, v. 5, p. 303–309, doi: 10.1111/j.1472-4669.2007.00130.x.

Xie, S., Pancost, R.D., Huang, J., Wignall, P.B., Yu, J., Tang, X., Chen, L., Huang, X., and Lai, X., 2007, Changes in the global carbon cycle occurred as two episodes during the Permian-Triassic crisis: *Geology*, v. 35, p. 1083–1086, doi: 10.1130/G24224A.1.

Manuscript received 10 March 2010

Revised manuscript received 15 June 2010

Manuscript accepted 22 June 2010

Printed in USA